Supplementary materials

Polyphenol-modified biomimetic bioadhesives for the therapy of annulus fibrosus defect and nucleus pulposus degeneration after discectomy

Yan Ju [a], *Shiyuan Ma* [a], *Meimei Fu* [a], *Min Wu* [a], *Yue Li* [a, b], *Yue Wang* [a], *Meihan Tao* [a,*], *Zhihui Lu* [a, c,*] *and Jinshan Guo* [a, c, d,*]

[a]Department of Histology and Embryology, NMPA Key Laboratory for Safety Evaluation of Cosmetics, School of Basic Medical Sciences, Guangdong Provincial Key Laboratory of Bone and Joint Degeneration Diseases, The Third Affiliated Hospital of Southern Medical University, Southern Medical University, Guangzhou 510515, P. R. China

[b]Department of Plastic and Aesthetic Surgery, Nanfang Hospital of Southern Medical University, Guangzhou, 510515, P. R. China

[c]Regenerative Medicine and Tissue Repair Material Research Center, Huangpu Institute of Materials, 88 Yonglong Avenue of Xinlong Town, Guangzhou, 511363, P. R. China

[d]CAS Key Laboratory of High-Performance Synthetic Rubber and its Composite Materials, Changchun Institute of Applied Chemistry, Chinese Academy of Sciences, 5625 Renmin Street, Changchun 130022, P. R. China

* Corresponding authors:

E-mails: jsguo4127@smu.edu.cn, guojinshan@ciac.ac.cn (Prof. J. Guo, Tel: +86-431-85264326), luzhihui@ciac.ac.cn (Prof. Z. Lu), taomeihan92@163.com (Dr. M. Tao).

Table S1. Primer sequences used in qRT-PCR

Primer	Sequence (forward 5'-3')	Sequence (reverse 5'-3')
Acan	CACTTTACTCTTGGTCTTTGTG	AGTGAGTTGTCATGGTCTG
Col-II	GTTCACGTACACTGCCCTGA	TGTCCATGGGTGCAATGTCA
Mmp-13	ATACGAGCATCCATCCCGAGACC	AACCGCAGCACTGAGCCTTTTC
Timp-1	CCACCTTATACCAGCGTT	AGAGAAAGAAAGATGGAGGA
Adamts-4	GCTTCGCTTCGCTGAGTAGA	GGTTTCGGATGCTTGGATGC
β-actin	TCAGGTCATCACTATCGGCAAT	AAAGAAAGGGTGTAAAACGCA

Table S2. Pfirrmann Grading System [1].

Grade	Structural changes within NP	Signal intensity	Intervertebral disc height
I	Homogenous and bright	Hyperintense	Normal
II	Heterogenous	Intermediate	Normal
III	Heterogenous and gray	Intermediate	Decreased
IV	Heterogenous and black	Hypointense	Decreased or collapsed

28 **Table S3.** Thompson Score System [2].

29

30

Grade	Nucleus	Anulus	End-plate	Vertebral body
I	Bulging gel	Discrete fibrous lamellas	Hyaline, uniformly thick	Margins rounded
II	White fibrous tissue peripherally	Mucinous material between lamellas	Thickness irregular	Margins pointed
III	Consolidated fibrous tissue	Extensive mucinous infiltration; loss of anular-nuclear demarcation	Focal defects in cartilage	Early chondrophytes or osteophytes at margins
IV	Horizontal clefts parallel to end-plate	Focal disruptions	Fibrocartilage extending from subchondral bone; irregularity and focal sclerosis in subchondral bone	Osteophytes less than 2 mm
V	Clefts extend through nucleus and anulus		Diffuse sclerosis	Osteophytes greater than 2 mm

Table S4. Degeneration grading system for rat intervertebral discs (IVDs) [3].

Category	Features	Score	Description
NP morphology	NP shape	0	Round/oval shape
		1	Round/oval with mild distortion
		2	Irregular shape
	NP area	0	NP constitutes more than 40% of disc area
		1	NP constitutes 40% to 20% of disc area
		2	NP constitutes less than 20% of disc area
NP cellularity	Cell number	0	Normal number of nuclear cells (NP cells comprise more than 2/3 of NP space)
		1	Slight decrease in number of cells (NP cells comprise 2/3 to 1/3 of NP space)
		2	Moderate or severe decrease in number of cells (NP cells comprise less than 1/3 of NP space)
	Cell morphology	0	More than 80% of nuclear cells are large and vacuolated
		1	80% to 30% of nuclear cells are large and vacuolated
		2	Less than 30% of nuclear cells are large and vacuolated
NP-AF border	Border appearance	0	Normal, clear distinction between NP and AF
		1	Minimal interruption, loss of distinction between NP and AF
		2	No distinction between NP and AF
AF morphology	Lamellar organization	0	Discrete, well-organized collagen lamellae bulging outward (less than 20% of annular lamellae are infolding, distorted, disorganized or serpentined)
		1	20% to 60% of annular lamellae are infolding, distorted, disorganized or serpentined
		2	More than 60% of annular lamellae are infolding, distorted, disorganized or serpentined
	Tears/fissures/disruptions	0	No ruptured fibers
		1	Ruptured fibers in less than 1/3 of the anulus
		2	Ruptured fibers in more than 1/3 of the anulus
Endplate	Disruptions/ microfractures and osteophyte/ ossification	0	Continuous endplate with no osteophyte or endplate ossification
		1	Endplate with minimal disruption (<1/3), mild osteophyte or mild endplate ossification (<1/3)
		2	Endplate with moderate or severe disruption (≥1/3), overgrowth of osteophyte or significant endplate ossification (≥1/3)

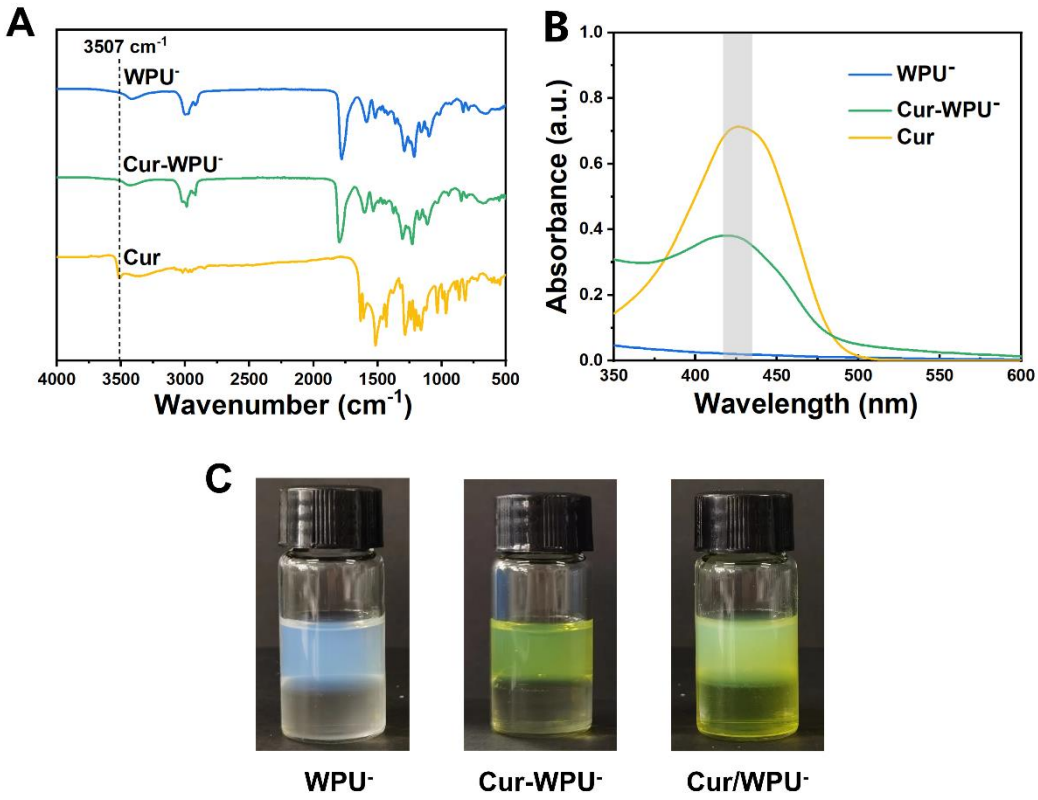

Fig. S1. Characterizations of Cur-WPU$^-$. (A) FTIR spectra and (B) UV-vis absorption spectra of WPU$^-$, Cur-WPU$^-$ and Cur. (C) Macroscopical migration of WPU$^-$, Cur-WPU$^-$ (chemical modification) and Cur/WPU$^-$ (physical blend) in aqueous phase and organic phase.

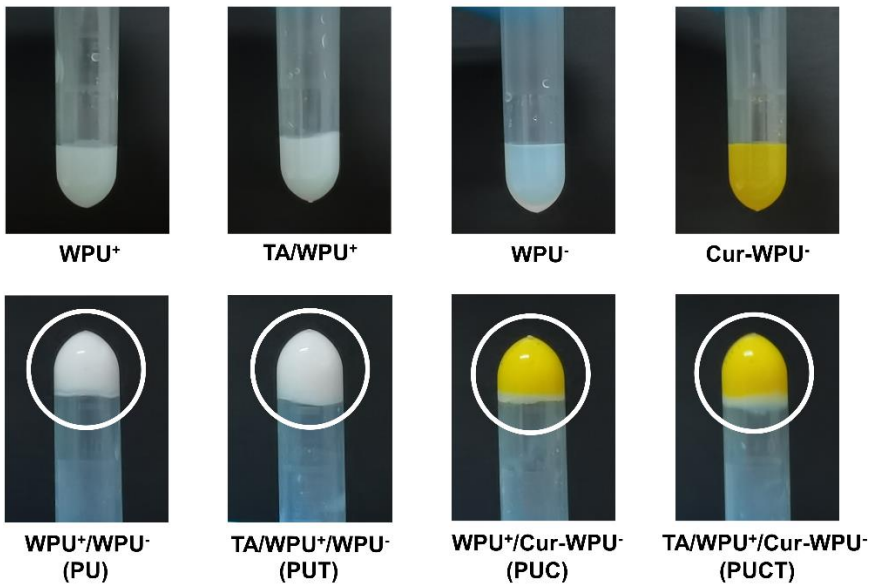

Fig. S2. Macroscopical images of single component and composite gelation.

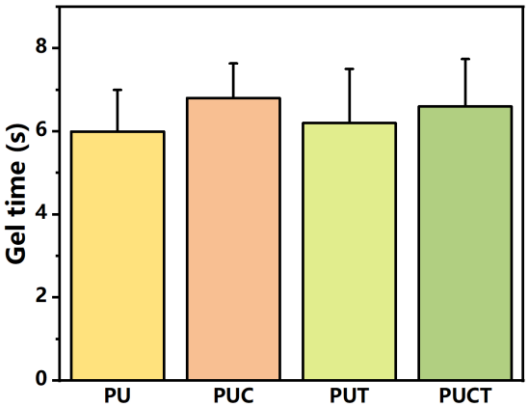

Fig. S3. Gel time of bioadhesives.

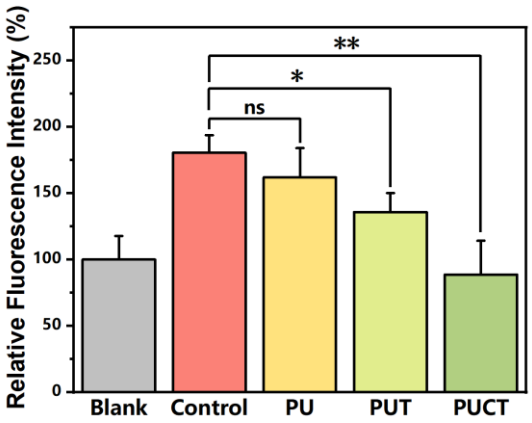

Fig. S4. The fluorescence intensities of ROS monitored via DCFH-DA probe in the NPCs. *$p < 0.05$, **$p < 0.01$; ns, no significant difference.

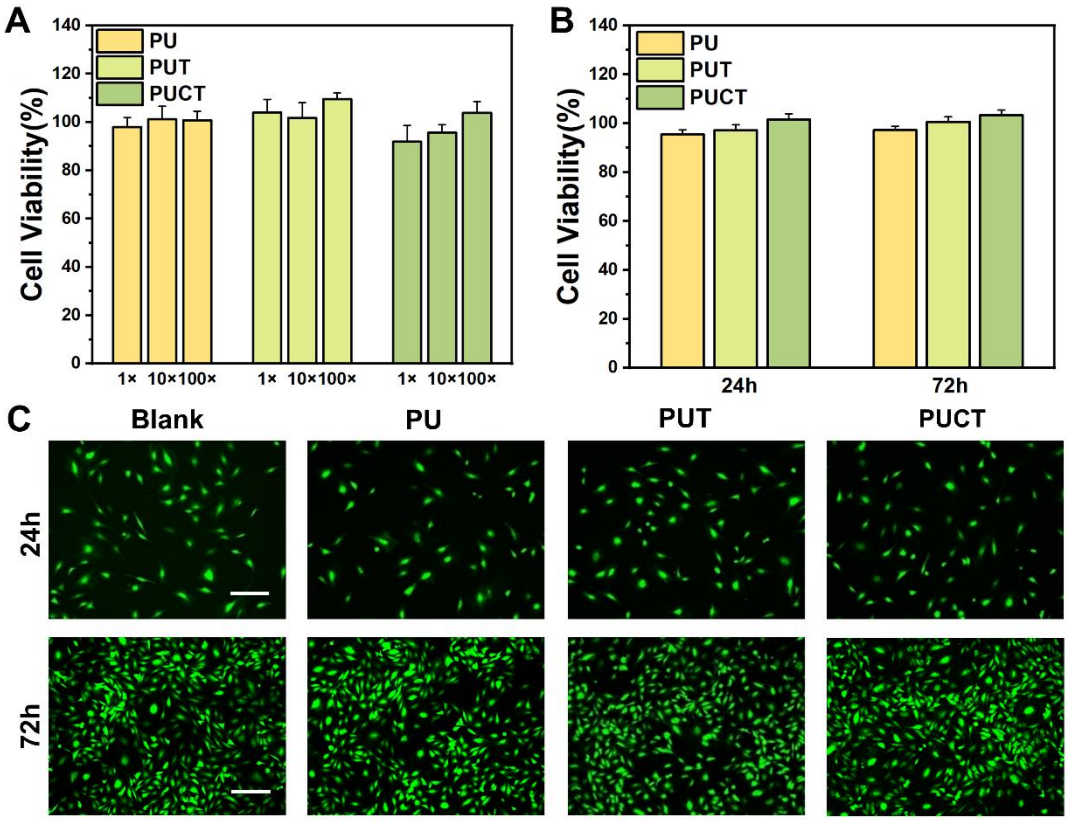

Fig. S5. *In vitro* cytotoxicity evaluation. CCK-8 assay analysis of the NPCs cultured with (A) medium extract of different diluted concentration (1×, 10×, 100×) for 24 h, and (B) PPU-glue for 24 h and 72 h. (C) Live/Dead staining images of the NPCs cultured with PPU-glue for 24 h and 72 h (scale bar = 200 μm).

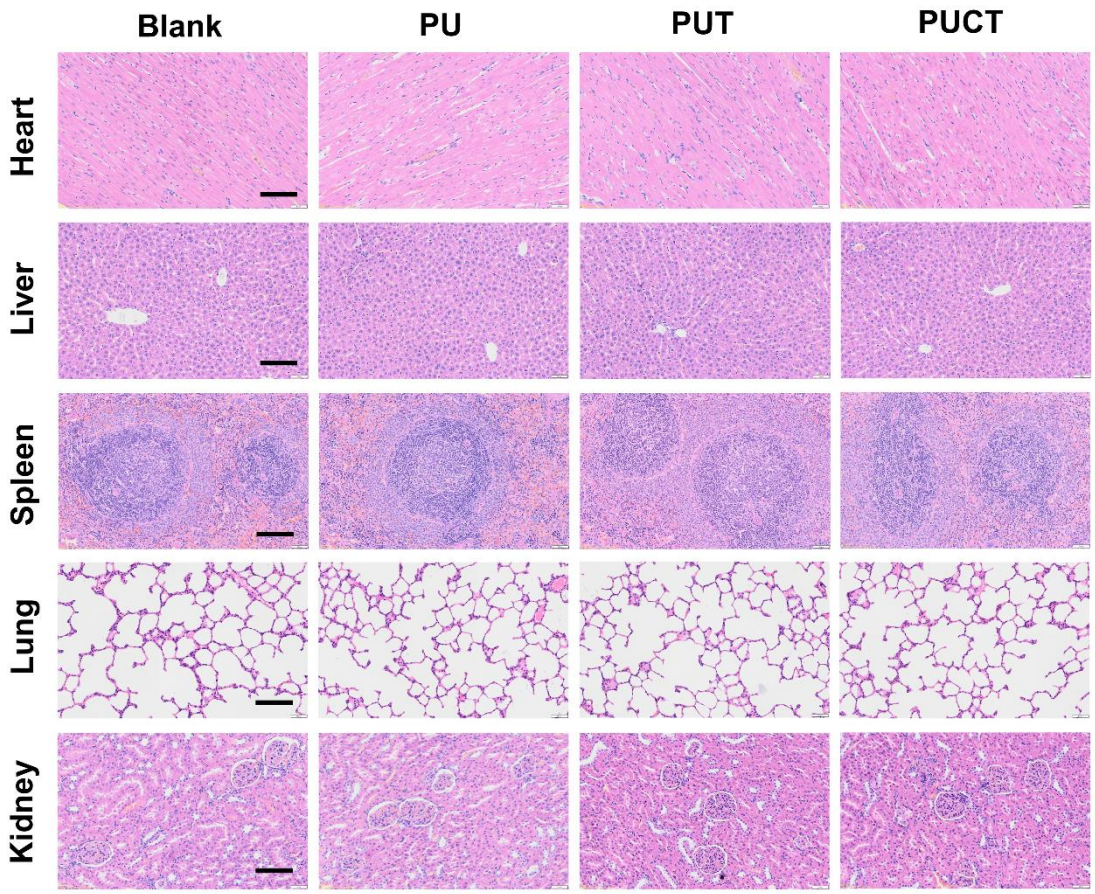

Fig. S6. *In vivo* organotoxicity evaluation. H&E staining of the heart, liver, spleen, lung and kidney tissue slices after 8-week treatment (scale bar = 100 μm).

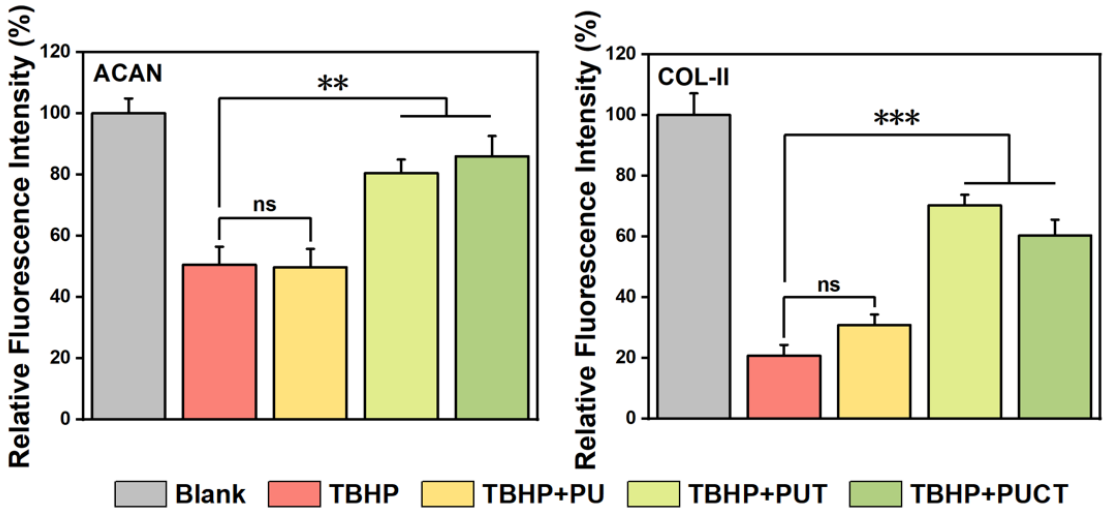

Fig. S7. The fluorescence intensities of ACAN and COL-II expressions in the NPCs.

$^{**}p < 0.01$, $^{***}p < 0.001$; ns, no significant difference.

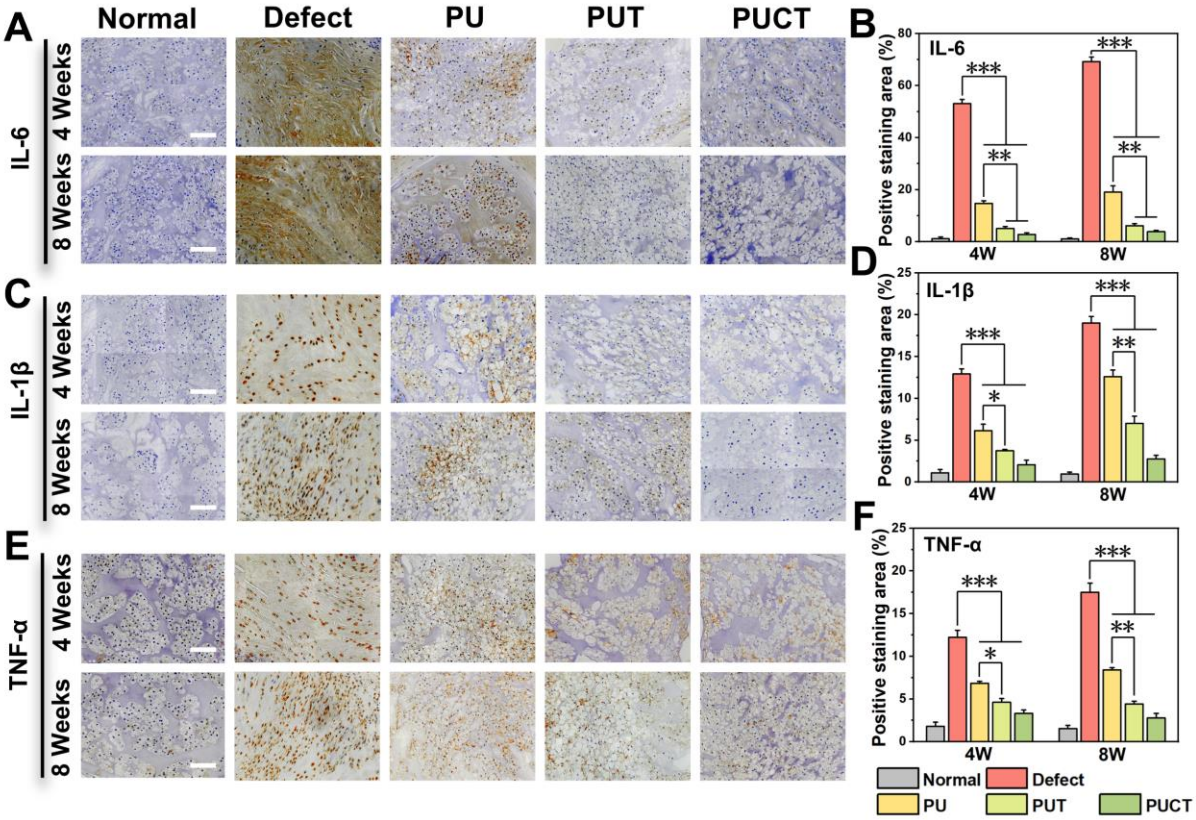

Fig. S8. Immunohistochemical analysis of NP inflammation at 4 and 8 weeks after surgery. The images and quantitative analysis of (A, B) IL-6, (C, D) IL-1β and (E, F) Tnf-α. Scale bar = 50 μm. *$p < 0.05$, **$p < 0.01$, ***$p < 0.001$.

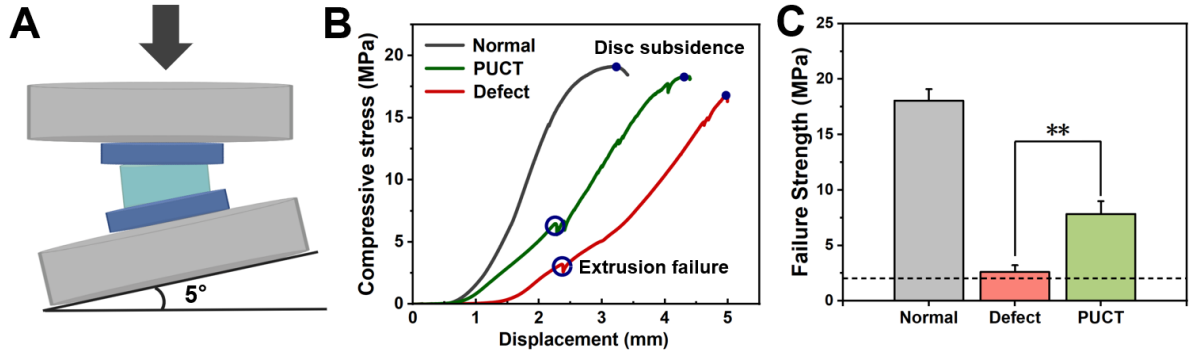

Fig. S9. *In vitro* biomechanical evaluation of AF seal. (A) Diagram of the ramp-to-failure tests performed on bovine tail discs. (B) The stress-displacement curves, showing extrusion failure (open circle) and disc subsidence (solid circle). (C) The failure strength. The dashed line represents the physiological upper bound of intradiscal pressure (2.3 MPa). $^{**}p < 0.01$.

References

[1] P. Grunert, B.H. Borde, S.B. Towne, Y. Moriguchi, K.D. Hudson, L.J. Bonassar, R. Haertl, Riboflavin crosslinked high-density collagen gel for the repair of annular defects in intervertebral discs: An in vivo study, Acta Biomater. 26 (2015) 215-224.

[2] J.P. Thompson, R.H. Pearce, M.T. Schechter, M.E. Adams, I.K. Tsang, P.B. Bishop, Preliminary evaluation of a scheme for grading the gross morphology of the human intervertebral disc, Spine 15(5) (1990) 411-415.

[3] A. Lai, J. Gansau, S.E. Gullbrand, J. Crowley, C. Cunha, S. Dudli, J.B. Engiles, M. Fusellier, R.M. Goncalves, D. Nakashima, J. Okewunmi, M. Pelletier, S.M. Presciutti, J. Schol, Y. Takeoka, S.D. Yang, T. Yurube, Y. Zhang, J.C. Iatridis, Development of a standardized histopathology scoring system for intervertebral disc degeneration in rat models: An initiative of the ORS spine section, JOR Spine 4(2) (2021) e1150.